Controller Hardware-in-the-Loop Testbed for Distributed Coordination and Control Architectures

Oscar Azofeifa, Siddhartha Nigam, Olaoluwapo Ajala, Christopher Sain, Samuel Utomi,
Alejandro D. Domínguez-García, Peter W. Sauer
ECE, University of Illinois at Urbana-Champaign
Email: {ora2, nigam4, ooajala2, sain2, sutomi2, aledan, psauer}@illinois.edu

***Abstract*—This paper describes a controller hardware-in-the-loop testbed that was developed to provide an ultra-high fidelity real-time environment for testing coordination and control architectures for distributed energy resources. Although the testbed is equipped to validate the effectiveness of architectures based on centralized, decentralized, and/or distributed decision-making algorithms, the focus of this paper is to describe a setup of the controller hardware-in-the-loop testbed that accommodates and facilitates the testing and validation of distributed coordination and control architectures. We provide results from case studies that utilize this setup.**

***Index Terms*—Controller hardware-in-the-loop testing, Distributed control, Distributed energy resources, Microgrids**

I. Introduction

The past decade has seen an increasing prevalence of distributed energy resources (DERs) in the electric power grid of numerous countries across the globe. Yet, as the underlying technologies improve, mature, and become more cost effective, DERs are projected to continue to experience a growing adoption rate [1]. As a result, several coordination and control architectures have been proposed for optimal utilization of DERs so as to maximize revenue and/or value for its stakeholders [2]–[5]. In addition, the microgrid concept has been posed as, and shown to be, a promising approach for effectively managing DERs (e.g., [6], [7]). A microgrid operating in grid-connected or islanded modes can be characterized by two layers [8]: (i) the physical layer, and (ii) the cyber layer. The physical layer is composed of the electrical infrastructure utilized for generation and distribution of electrical energy, and the cyber layer comprises the hardware and software for communication and control.

Recent efforts aimed at developing coordination and control architectures for the DERs in a microgrid are based on a centralized and/or decentralized decision-making approach [9]–[11]. However, these methodologies have underlying limitations that restrict either the functions or the potential practicality, as well as feasibility, of the resulting architecture [12]. For example, architectures based on a centralized decision-making approach are susceptible to a single point of failure, whereas those based on a decentralized decision-making approach typically lack the flexibility that is necessary for seamless integration of additional resources. An alternative approach for developing DER coordination and control architectures involves the use of a distributed decision-making scheme. In this approach, control and coordination decisions pertaining to each DER are based on local information acquired, e.g., from measurements and other information obtained through exchanges with neighboring DERs; this affords several unique advantages, including robustness, resiliency, scalability, and cost effectiveness [13]. As a result, this paper focuses on the development of a testbed for distributed coordination and control architectures.

Although it is crucial to validate the effectiveness of DER coordination and control architectures in real applications, the associated costs and resources limit the degree to which this can be practically realized—this mostly results from the need for a variety of test scenarios and operating conditions, and the use of hardware components that comprise the electric power system [14]–[16]. Hence, in an effort to overcome these limitations, we designed and built a controller hardware-in-the-loop (C-HIL) testbed. We developed ultra-high fidelity models of various components of the physical layer, i.e., DERs, distribution lines, and loads [17]–[19], implemented them on a high-resolution real-time emulation device [20], and interconnected our control hardware devices (the cyber nodes) to the real-time emulation device; the algorithms and protocols associated with the distributed coordination and control architecture are synthesized on each cyber node. In other words, any test system can be realized in the emulated physical layer, and its distributed coordination and control architecture can be realized in the actual cyber layer. As a result, our C-HIL testbed provides an effective, efficient, repeatable, low cost, scalable, and adjustable testing environment for distributed coordination and control architectures.

The remainder of this paper is organized as follows. In Section II, we describe the distributed coordination and control architecture that was tested and validated on our C-HIL testbed. In Section III, we provide a description of the testbed; we describe the cyber layer, the physical layer, and the graphical user interface used for visualization of the cyber layer. In Section IV, we report the use of this testbed for two studies. We provide some concluding remarks in Section V.

II. Architecture for DER Coordination

In this section, we describe a distributed coordination and control architecture that was tested and validated using our C-HIL testbed. The purpose of the architecture is to coordinate and control a group of DERs to collectively provide frequency regulation services to the bulk power grid—it is assumed that

the DERs are located within a microgrid and can exchange information with each other via some communication network. Firstly, we describe the distributed decision-making process that the architecture is based on, and afterwards we discuss the various well documented protocols and algorithms that facilitate the distributed decision making process (see [8] for a detailed description of the architecture). These algorithms and protocols, along with the cyber-physical components, form the C-HIL testbed.

A. DER Coordination and Control Process

A regulation signal, whose value is a function of the bulk power grid requirements, the distribution network constraints, and the DER capacity limits, is first of all determined by a system operator. The system operator transmits this information to an aggregator, and the aggregator forwards it to the cyber nodes it is connected to. Thereafter, by relying on a communication network, all cyber nodes exchange information with their neighboring nodes, iteratively, until each cyber node is able to compute desired generation setpoints for the DERs they are in command of—this information exchange and setpoint computation process is based on the use of a distributed decision-making algorithm.

B. Algorithms and Protocols

The decision-making algorithm at the core of the aforementioned distributed coordination and control architecture is called the ratio-consensus algorithm. The algorithm, which is described in [8], [21]–[24] in great detail, serves as a primitive for solving many coordination and control problems in a distributed fashion. In the ratio-consensus algorithm, each cyber node i maintains two internal states y_i and z_i, which, at iteration k, it updates and broadcasts to its neighboring cyber nodes. The values of y_i and z_i at instant k, denoted by $y_i[k]$ and $z_i[k]$, respectively, are used to compute $\gamma_i[k] = \frac{y_i[k]}{z_i[k]}$, and after a finite number of iterations K, which can be determined as described in [25], the resulting $\gamma_i[k]$ is close to $\frac{\sum_i y_i[0]}{\sum_i z_i[0]}$ for all i and all $k > K$. A variant of this algorithm, called the robust ratio-consensus algorithm, is proposed in [2], [26], and as the name suggests, it is robust against packet drops in the communication links.

Before an offline cyber node (a node that is not connected to the distributed communication network) can take part in ratio-consensus executions, its internal clock must be synchronized to the common time reference of all online cyber nodes, i.e., nodes that are connected to the communication network. As a result, we developed a time resynchronization protocol for synchronization of an offline cyber node's clock to the common time reference of the cyber layer. The protocol is a variant of the clock synchronization protocol that was described in [8].

The time resynchronization protocol is executed by each online cyber node immediately after an execution of the ratio-consensus algorithm. When this happens, each online node broadcasts a "resync" package and stores the broadcast time t_1. Each "resync" package contains information on the offset between the online cyber node's clock and the common time reference; we refer to this as the global offset d_g. When an offline cyber node receives a "resync" package, it stores d_g and the package receipt time t_2, and at time t_3, it sends a response package that contains information on t_2 and t_3. The online node receives the response message at time t_4 and now it has all the necessary information to compute the local offset d_l as follows:

$$d_l = \frac{(t_2 - t_1) - (t_4 - t_3)}{2}. \tag{1}$$

The online cyber node sends a package containing information on d_l to the offline cyber node, and the offline node computes

$$d = d_g + d_l, \tag{2}$$

which is the offset between the offline nodes clock and the common time reference. This value is used to synchronize the clock of the offline cyber node to the common time reference of the online cyber nodes.

III. Testbed

This section describes the underlying hardware and software infrastructure that constitutes our C-HIL testbed. A brief description of the cyber layer infrastructure, the physical layer infrastructure, and the graphical user interface, which is utilized for visualization of the cyber layer, is provided.

A. Cyber Layer Infrastructure

As depicted in Fig. 1, n control hardware devices, which we refer to as cyber nodes, and a virtual entity, which we refer to as an aggregator, make up the cyber layer. The aggregator serves as an intermediary between the cyber nodes and a higher-level authority, e.g., the bulk power system operator. These cyber layer components implement the algorithms and protocols that realize the distributed coordination and control architecture discussed earlier.

Each cyber node is composed of an Arduino Due. Neighboring cyber nodes communicate wirelessly via a MaxStream XB24-DMCIT-250 revB XBee wireless module that is interfaced to the Arduino Due. Also, using an Ethernet shield model W5100 that is connected to the Arduino Due, each cyber node communicates with several lower-level controllers via Ethernet.

Two standard protocols were implemented to facilitate communication between the cyber nodes, as well as between each cyber node and several lower-level controllers: (1) Zigbee protocol for peer-to-peer wireless communication between cyber nodes, and (2) Modbus TCP/IP protocol for Ethernet communication between each cyber node and the lower-level controllers. Communication between the aggregator and the cyber nodes is achieved via a serial communication protocol.

B. Physical Layer Infrastructure

In our C-HIL testbed setup, the physical layer is emulated using either a Typhoon HIL real-time simulator or the Open Distribution System Simulator. Also, lower-level

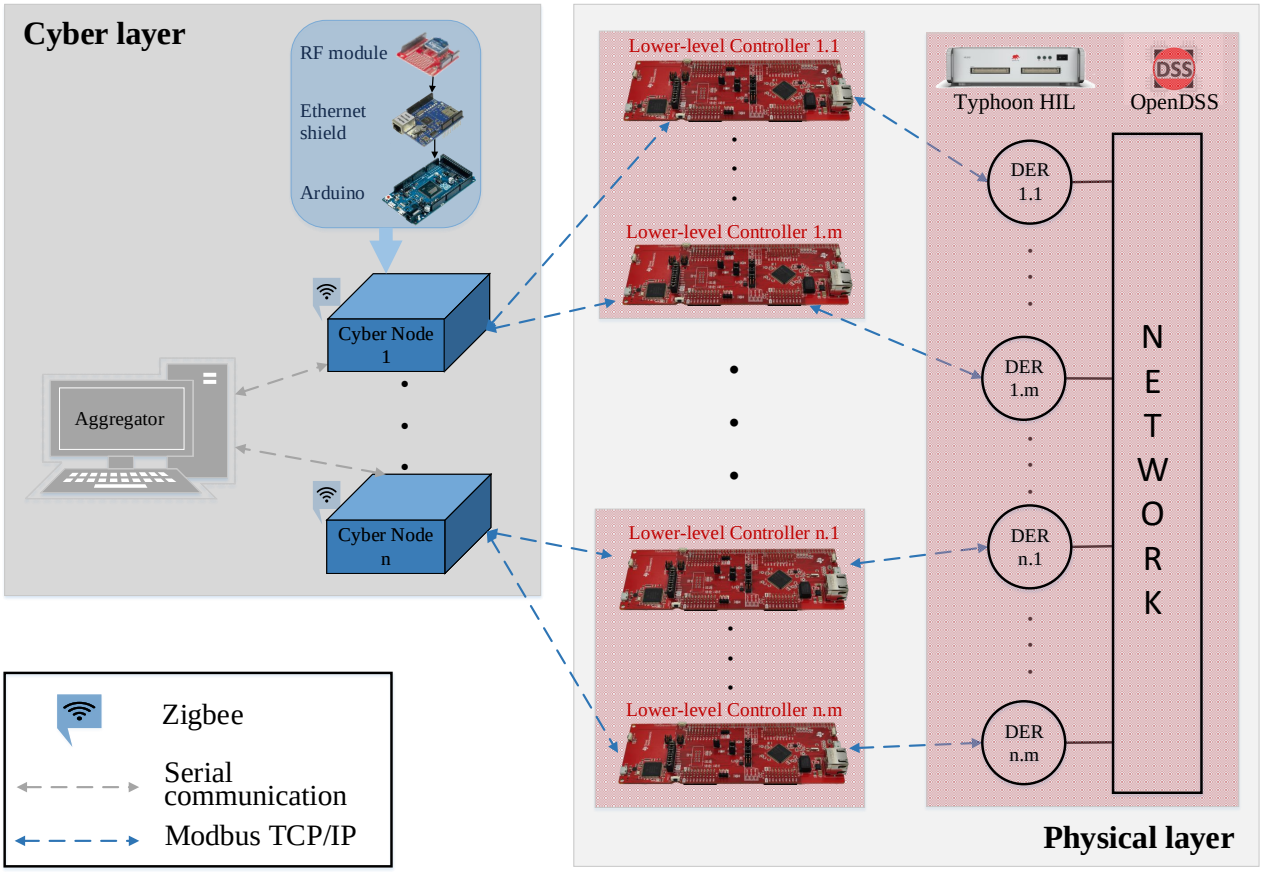

Fig. 1: A Schematic of the Controller Hardware-in-the-Loop Testbed.

control schemes for each DER are synthesized on a controller hardware device.

1) Typhoon HIL Hardware: The C-HIL testbed is equipped with three ultra-high fidelity real-time simulation hardware devices: one Typhoon HIL 402 and two Typhoon HIL 603s. By allowing real-time simulation step sizes as low as 0.5 μs, PWM sampling of 20 ns, and implementing very detailed models of system components, as discussed in [19], these devices accurately emulate the effects of switching transients and electromagnetic transients on the electric power system. Reduced-order models proposed in [17]–[19] are also implemented on the Typhoon HIL devices to reduce the modeling complexity and, as a result, lower the computational cost of emulating a large number of DERs.

2) Open DSS Software: The testbed is equipped with a software developed by the Electric Power Research Institute (EPRI) called Open Distribution System Simulator (OpenDSS) (see [27] for a detailed description of the software). We utilize the OpenDSS software in our C-HIL testbed because of its capacity to emulate large distribution networks, its adaptability for cosimulation, its high usability, and the large number of publicly available standard distribution network models that have been developed in OpenDSS. In our C-HIL testbed, the OpenDSS software is executed on an off-the-shelf desktop computer.

3) Lower-level Controller Hardware: The C-HIL testbed is equipped with multiple Texas Instruments MSP-EXP432e401y Ethernet boards for implementation of lower-level DER control schemes such as governor control, frequency droop control, voltage droop control, and virtual oscillator control. As shown in Fig. 1, a bidirectional communication link is established between each cyber node and m lower-level controllers, as well as between each lower-level controller and the simulation device. The Modbus TCP/IP protocol is employed.

C. Graphical User Interface

A graphical user interface (GUI) was developed for real-time monitoring of the cyber layer. For this purpose, we made use of Processing Integrated Development Environment (IDE) [28]. This IDE is based on Java and provides access to libraries that ease the creation of interactive visualization tools.

The GUI visualizes information in three different modes: (i) graph mode, (ii) communication mode, and (iii) plot mode. The graph mode displays the graph associated with the communication network. The communication mode displays the network in a more dynamic fashion than that in Graph mode. The plot mode displays data of the iterative process in real time after each round of the distributed algorithm execution.

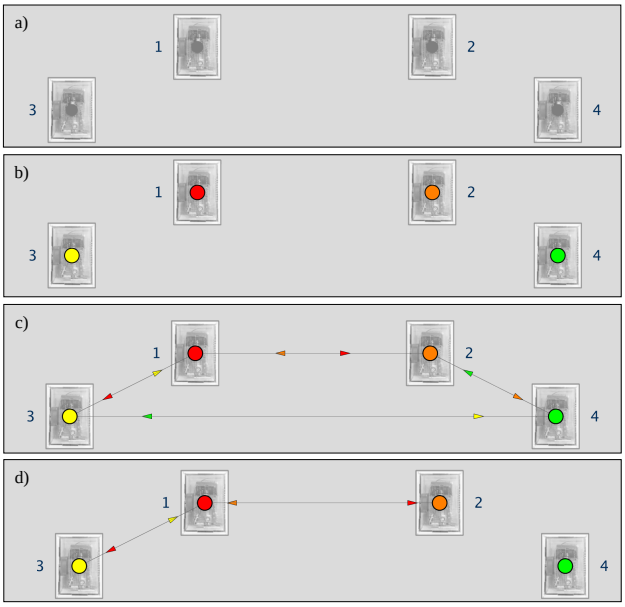

Fig. 2: GUI in Communication mode for 4 cyber nodes network.

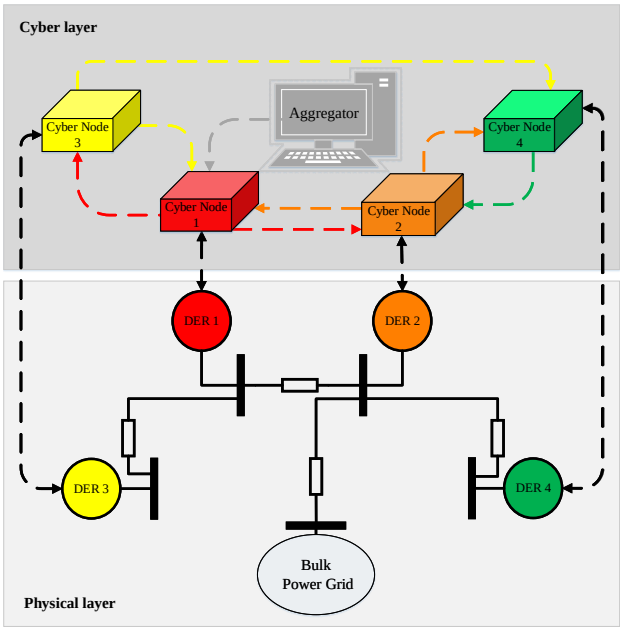

Fig. 3: Cyber-physical representation of a grid-connected microgrid.

A key use of the GUI is to monitor two different failure modes that may occur in the cyber layer: (i) link failure, and (ii) node failure. A link failure is a communication failure between two neighboring cyber nodes, and it is caused by loss of data (packet drops) during the send/receive process. A link failure is modeled in the GUI by a communication link disappearing from the graph. A node failure could be caused by a cyber node being physically disconnected from the network (node down), or by a cyber node going offline, as described in Section II-A. In the GUI, these two modes, i.e., node down and node offline, are visualized differently. A node down is visualized by hiding the corresponding visual representation of the node in the graph, whereas a node offline is visualized by eliminating all links connecting the offline node to its neighbors.

A snapshot of the GUI in communication mode is shown in Fig. 2. Panel a) of the figure shows the network in its initial configuration, when all cyber nodes are offline. As shown in panel b), when the cyber nodes are identified by the GUI application, they are visualized as color-coded circles, to distinguish each cyber node. After the cyber nodes are synchronized, an animation of moving arrows appears to represent the communication links between neighbors as well as the communication direction; this is depicted in panel c). Panel d) depicts the GUI when node 4 goes offline.

IV. Case Studies

Using two case studies, this section demonstrates the capabilities of the C-HIL testbed for the testing and validation of the aforementioned distributed coordination and control architecture. We provide details on the setup of the testbed for the testing and validation tasks, pointing out the different components of the testbed used in each case study. The first case study comprises a four-node microgrid connected to the bulk grid, whereas the second case study comprises the University of California San Diego Microgrid connected to the bulk power grid.

A. 4-bus Microgrid Providing Frequency Regulation Services to the Bulk Grid

Figure 3 portrays a cyber-physical representation of a grid-connected microgrid that is equipped with a distributed coordination and control architecture. This case study makes use of the synthetic four DER microgrid case depicted in Fig. 3, with each DER being a battery storage system.

The goal of this case study is to coordinate and control the response of the DERs so that the microgrid's active power injection into the bulk grid tracks a frequency regulation signal sent from the aggregator. Each DER was modeled on a Typhoon HIL 402 using ultra-high fidelity models of a LCL filter, a three phase inverter, and a battery storage unit (see [19] for modeling details). In this setup, each cyber node controls a DER in the Typhoon HIL, and the lower-level control scheme for each DER was emulated in the Typhoon HIL 402 (i.e., the lower-level controller hardware was not used). The aggregator was used to send continuous frequency regulation signals to one cyber node, referred to as the leader node, and the cyber layer utilized the distributed coordination and control architecture in order to compute desired regulation signals for each DER modeled in the Typhoon HIL 402. The PJM RegD test signal [29] was utilized for this study.

PJM's performance compliance for frequency regulation service defines a metric called the performance score, and each participating DER or microgrid is required to have a performance score greater than 75% [30]. The results from this study are shown in Fig. 5. After comparing the regulation sig-

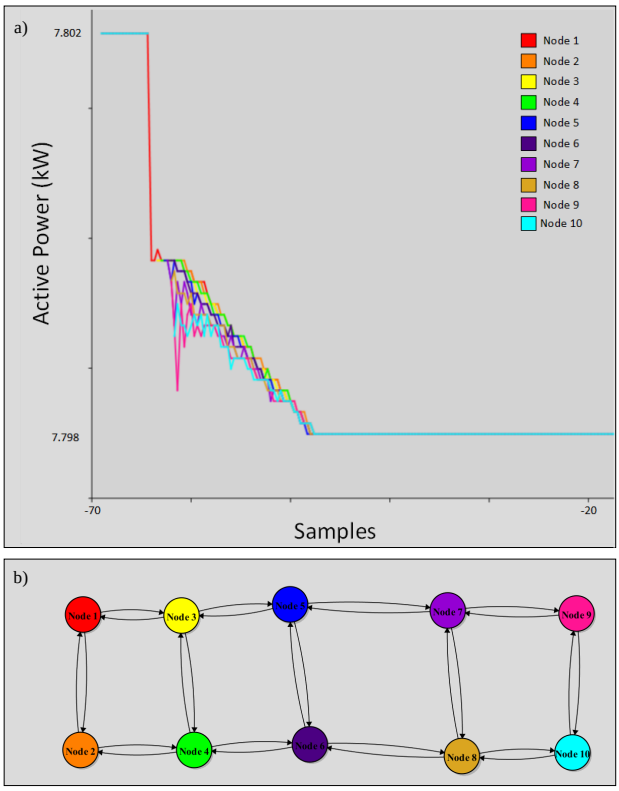

Fig. 4: GUI in Plot mode and Graph mode.

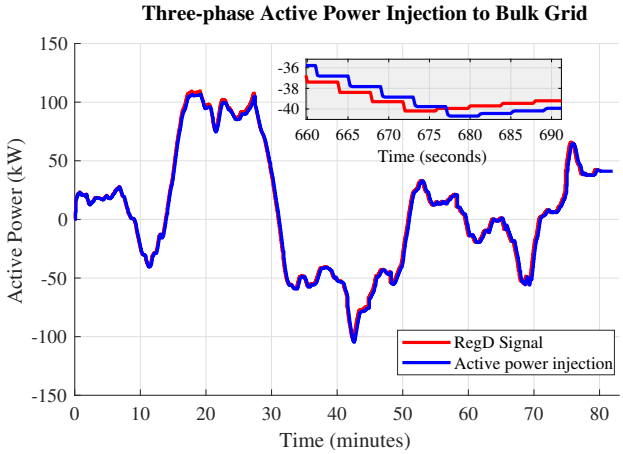

Fig. 5: PJM RegD Signal Response in first case.

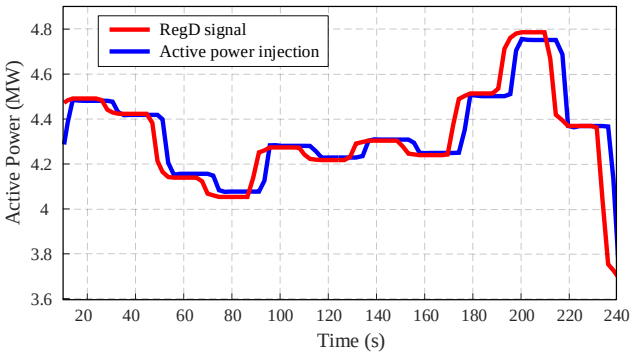

Fig. 6: PJM RegD Signal Response in second case.

nal to the microgrid active power injection into the bulk grid, and accounting for the delays introduced by the distributed coordination and control architecture, a performance score of 89.2% was computed for the microgrid.

B. The UCSD Microgrid Providing Frequency Regulation Services to the Bulk Grid

The University of California San Diego (UCSD) microgrid has 100 controllable nodes comprising 10 photovotaic (PV) generators, 3 gas and steam turbines, and 87 loads (buildings and electric vehicle (EV) charging stations). Additionally, there are 20 uncontrollable loads in the system. The loads and generators are interconnected via a network of distribution lines and 52 transformers to the bulk grid, at a 69kV voltage level. The goal of this case study is to coordinate and control the DERs and controllable loads such that the UCSD microgrid's active power injection to the bulk grid tracks a frequency regulation signal sent by the aggregator.

We made use an OpenDSS reduced-model of the UCSD microgrid obtained using the method developed in [31], and implemented the primary control schemes of each DER on a lower-level controller hardware device. Although OpenDSS is not a real-time simulator, we mimicked a real-time operation by polling the OpenDSS results continuously and implementing appropriate delays on the results. The regulation signal was sent to one of the cyber nodes from the aggregator, and afterwards the cyber layer utilized the distributed coordination and control framework described in Section II to compute desired regulation signals for each DER modeled in the OpenDSS. Figure 4 depicts a snapshot of the GUI during the execution of this case. Panel a) of the figure shows the GUI in plot mode for one execution of the distributed algorithm. Panel b) of the figure shows the GUI in graph mode for the cyber network representation.

A five-minute long frequency regulation signal from PJM was used in this case study, and we used standard metrics to validate the corresponding results. In particular, we required that: (i) initial response time < 5 s, (ii) reserve magnitude target $> 5\%$, (iii) reserve magnitude variability $\leq \pm 5\%$, (iv) ramp time ≤ 5 min, (v) duration $>= 30$ min, and (vi) availability $> 95\%$. The results are presented in Fig. 6. The UCSD microgrid's active power is shown to track the frequency regulation signal, and we showed that the required performance metrics were met. Figure 6 shows a response delay of approximately 4.5 s. The delay is caused by the time taken to implement the distributed coordination and control architecture.

V. Concluding Remarks

In this paper, we reported the development of a controller hardware-in-the-loop testbed for the testing and validation of

distributed coordination and control architectures. The presented case studies highlight two capabilities of the testbed: (1) the ability to accommodate the use of ultra-high fidelity models of DERs, and (2) the interfacing capability of the testbed with other third party platforms, such as EPRI's OpenDSS, in order to accommodate testing on large test systems.

VI. Acknowledgement

The authors would like to thank Manasa Muralidharan, Oytun Babacan, Zachary Pecenak, Hamed Valizadeh Haghi, and Jan Kleissl for creating and providing us with an OpenDSS model of the UCSD microgrid.

References

[1] North American Electric Reliability Corporation, "Distributed energy resources connection modeling and reliability considerations," Tech. Rep., 2017.

[2] A. D. Domínguez-García, C. N. Hadjicostis, and N. Vaidya, "Resilient networked control of distributed energy resources," *IEEE Journal on Selected Areas in Comm.*, vol. 30, no. 6, pp. 1137–1148, July 2012.

[3] D. Bakken, A. Bose, K. M. Chandy, P. P. Khargonekar, A. Kuh, S. Low, A. von Meier, K. Poolla, P. P. Varaiya, and F. Wu, "Grip - grids with intelligent periphery: Control architectures for grid2050$^{\pi}$," in *Proc. of the IEEE International Conference on Smart Grid Communications*, Oct. 2011, pp. 7–12.

[4] E. Mayhorn, L. Xie, and K. Butler-Purry, "Multi-time scale coordination of distributed energy resources in isolated power systems," *IEEE Transactions on Smart Grid*, vol. 8, no. 2, pp. 998–1005, Mar. 2017.

[5] D. B. Arnold, M. D. Sankur, M. Negrete-Pincetic, and D. S. Callaway, "Model-free optimal coordination of distributed energy resources for provisioning transmission-level services," *IEEE Transactions on Power Systems*, vol. 33, no. 1, pp. 817–828, Jan. 2018.

[6] R. H. Lasseter, "Microgrids," in *Proc. of the Power Engineering Society Winter Meeting*, vol. 1, 2002, pp. 305–308 vol.1.

[7] R. Arghandeh, M. Brown, A. Del Rosso, R. Ghatikar, E. Stewart, A. Vojdani, and A. Meier, "The local team leveraging distributed resources to improve resilience," *IEEE Power and Energy Magazine*, vol. 12, pp. 76–83, 09 2014.

[8] S. T. Cady, A. D. Domínguez-García, and C. N. Hadjicostis, "A distributed generation control architecture for islanded ac microgrids," *IEEE Transactions on Control Systems Technology*, vol. 23, no. 5, pp. 1717–1735, Sep. 2015.

[9] R. Zamora and A. K. Srivastava, "Controls for microgrids with storage: Review, challenges, and research needs," *Renewable and Sustainable Energy Reviews*, vol. 14, no. 7, pp. 2009 – 2018, 2010.

[10] N. L. Díaz, A. C. Luna, J. C. Vasquez, and J. M. Guerrero, "Centralized control architecture for coordination of distributed renewable generation and energy storage in islanded ac microgrids," *IEEE Transactions on Power Electronics*, vol. 32, no. 7, pp. 5202–5213, July 2017.

[11] A. Tuckey, S. Zabihi, and S. Round, "Decentralized control of a microgrid," in *Proc. of the European Conference on Power Electronics and Applications*, Sep. 2017, pp. P.1–P.10.

[12] A. D. Domínguez-García, *Coordination of Distributed Energy Resources for Provision of Ancillary Services: Architectures and Algorithms*. London: Springer London, 2013, pp. 1–8.

[13] A. D. Domínguez-García and C. N. Hadjicostis, "Coordination and control of distributed energy resources for provision of ancillary services," in *Proc. of the First IEEE International Conference on Smart Grid Communications*, Oct. 2010, pp. 537–542.

[14] C. S. Edrington, M. Steurer, J. Langston, T. El-Mezyani, and K. Schoder, "Role of power hardware in the loop in modeling and simulation for experimentation in power and energy systems," *Proc. of the IEEE*, vol. 103, no. 12, pp. 2401–2409, Dec. 2015.

[15] E. Limpaecher, R. Salcedo, E. Corbet, S. Manson, B. Nayak, and W. Allen, "Lessons learned from hardware-in-the-loop testing of microgrid control systems," in *Proc. of the Grid of the Future Symposium Cleveland, Ohio*, Oct. 2017. [Online]. Available: https://selinc.com/

[16] P. Kotsampopoulos, D. Lagos, N. Hatziargyriou, M. O. Faruque, G. Lauss, O. Nzimako, P. Forsyth, M. Steurer, F. Ponci, A. Monti, V. Dinavahi, and K. Strunz, "A benchmark system for hardware-in-the-loop testing of distributed energy resources," *IEEE Power and Energy Technology Systems Journal*, vol. 5, no. 3, pp. 94–103, Sep. 2018.

[17] O. Ajala, "A hierarchy of microgrid models with some applications," Ph.D. dissertation, University of Illinois at Urbana-Champaign, 2018.

[18] O. Ajala, A. D. Domínguez-García, and P. W. Sauer, *A Hierarchy of Models for Inverter-Based Microgrids*. New York, NY: Springer New York, 2018, pp. 307–332.

[19] O. Ajala, M. Almeida, I. Celanovic, P. W. Sauer, and A. D. Domínguez-García, "A hierarchy of models for microgrids with grid-feeding inverters," in *Proc. of the IREP Bulk Power System Dynamics and Control Symposium*, Aug. 2017.

[20] Typhoon hil 402 brochure. Typhoon HIL.

[21] A. D. Domínguez-García and C. N. Hadjicostis, "Distributed algorithms for control of demand response and distributed energy resources," in *Proc. of the IEEE Conference on Decision and Control*, 2011, pp. 27–32.

[22] S. T. Cady, A. D. Domínguez-García, and C. N. Hadjicostis, "Robust implementation of distributed algorithms for control of distributed energy resources," in *Proc. of the North American Power Symposium*, 2011, pp. 1–5.

[23] A. D. Domínguez-García, S. T. Cady, and C. N. Hadjicostis, "Decentralized optimal dispatch of distributed energy resources," in *Proc. of the IEEE Conference on Decision and Control*, 2012, pp. 3688–3693.

[24] B. A. Robbins, C. N. Hadjicostis, and A. D. Domínguez-García, "A two-stage distributed architecture for voltage control in power distribution systems," *IEEE Transactions on Power Systems*, vol. 28, no. 2, pp. 1470–1482, May 2013.

[25] S. T. Cady, A. D. Domínguez-García, and C. N. Hadjicostis, "Finite-time approximate consensus and its application to distributed frequency regulation in islanded ac microgrids," in *Proc. of the Hawaii International Conference on System Sciences*, Jan. 2015, pp. 2664–2670.

[26] C. N. Hadjicostis, N. Vaidya, and A. D. Domínguez-García, "Robust distributed average consensus via exchange of running sums," *IEEE Transactions on Automatic Control*, vol. 61, no. 6, pp. 1492–1507, June 2016.

[27] "Simulation tool: OpenDSS," Electric Power Research Institute (EPRI). [Online]. Available: http://smartgrid.epri.com/SimulationTool.aspx

[28] C. Reas and B. Fry, *Processing: A Programming Handbook for Visual Designers and Artists*. MIT Press, 2014.

[29] PJM. (2019, Mar.) Normalized signal test: RegD. [Online]. Available: https://www.pjm.com/markets-and-operations/ancillary-services.aspx

[30] ——, *PJM manual 12*, 2019. [Online]. Available: https://www.pjm.com/-/media/documents/manuals/m12.ashx

[31] Z. K. Pecenak, V. R. Disfani, M. J. Reno, and J. Kleissl, "Inversion reduction method for real and complex distribution feeder models," *IEEE Transactions on Power Systems*, vol. 34, no. 2, pp. 1161–1170, Mar. 2019.